Scientia Iranica C (2020) 27(3), 1234–1242

Sharif University of Technology
Scientia Iranica
Transactions C: Chemistry and Chemical Engineering
http://scientiairanica.sharif.edu

A kinetic study of acetone acidic oxidation with $KMnO_4$ in the absence and presence of CuO/γ-Al_2O_3 as a heterogeneous nano-catalyst

M.T. Badri[a], M. Barati[b], and S.H. Rasa[a,*]

a. *Department of Physical Chemistry, Faculty of Chemistry, University of Kashan, Kashan, Iran.*
b. *Department of Applied Chemistry, Faculty of Chemistry, University of Kashan, Kashan, Iran.*

Received 23 February 2019; received in revised form 10 September 2019; accepted 11 January 2020

KEYWORDS
Acetone oxidation;
Reaction kinetics;
Heterogeneous nano-catalyst;
CuO;
γ-Al_2O_3;
Reaction rate law.

Abstract. A kinetic study of acetone acidic oxidation with aqueous $KMnO_4$ in the absence and presence of CuO nanocatalysts was carried out. The rate laws and activation energies were evaluated in case of reaction with no catalyst and with 0, 2.5, 5, and 10 wt.% of CuO on γ-Al_2O_3. Catalysts were prepared by the impregnation method and characterized by ICP-OES, XRD, BET, and TEM. Products were analyzed with UV-VIS and examinations were performed by changing concentrations of a reactant and keeping the rest constant to determine the order of the reaction for the targeted one. Results showed that, in the absence and presence of nano-catalysts, the order of the reaction for all $KMnO_4$, $(CH_3)_2CO$, and H_2SO_4 was one. The rate constants for the reaction in the absence of catalyst and in the presence of 0, 2.5, 5 and 10 wt% CuO were 0.0022, 0.0023, 0.0025, 0.0026, and 0.0029 $L^2.mole^{-2}.min^{-1}$; in addition, the activation energies for them were 56.767, 56.807, 53.978, 50.075, and 46.774 $kJ.mol^{-1}$, respectively. Moreover, there was no relationship between the product concentrations and the rate of reaction. Therefore, the results showed that CuO on γ-Al_2O_3 had a significant effect on the reaction kinetics and can be a reliable heterogeneous catalyst for it.

1. Introduction

Acetone is a very useful material in many chemical and non-chemical industries. It is used as solvent and reagent for many reactions such as synthesis of methyl-methacrylate and bisphenol-A, which are both intensive products. It also has medical, cosmetic, and domestic uses. However, the presence of acetone as a toxic, colorless, volatile and flammable liquid in the aqueous and gaseous wastes of these industries causes environmental problems [1–3]. It has been demonstrated that acetone inhalation can negatively affect the central nervous system of humans, and also its anticonvulsant effect has been proven for the model animal [4].

Recently, environmental problems have become the reason for researchers to pay closer attention to acetone oxidation in gaseous and aqueous media and to the optimization of this process. In the gaseous medium, the process has proceeded in the presence of different catalysts such as platinum, palladium, cobalt, copper, nickel, and manganese [5–9]. Many chemical industrial reactions are run in the presence of solid catalysts. To increase the exposed surface area, the catalyst is commonly distributed on the surface of a porous support (or carrier). Common supports include silica gel (SiO_2), alumina (Al_2O_3),

*. *Corresponding author.*
E-mail address: Rasa@Kashanu.ac.ir (S.H. Rasa)

doi: 10.24200/sci.2020.53013.3006

carbon (in the form of charcoal), and diatomaceous earth. The support may be inert or may contribute to catalytic activity [10–12]. In a liquid medium, the oxidation of organic compounds in the presence of potassium permanganate has been widely investigated. Aqueous acetone oxidation has also been performed in the presence of $KMnO_4$ in different conditions.

Metallic copper and its different oxidation states have been used as catalysts for the oxidation of organic compounds. They are highly effective in carbon monoxide oxidation in different conditions [13,14]. The performance of CuO/Cu_2O nanoparticles as the electro-catalyst of formaldehyde oxidation in the liquid phase has been studied. Results have introduced these nanoparticles as promising catalysts for formaldehyde oxidation [15]. The oxidation of hydrogen peroxide has been carried out on the CuO/zeolite nano-catalyst. The effect of CuO loading on the performance of the nano-catalyst has been investigated. Results showed more oxidation levels up to 100% for higher loadings of CuO on zeolite [16]. The copper (II) oxide was used for acetone gas sensing based on acetone oxidation reaction at the operation temperatures of 200–360°C. Results showed that, in such a condition, CuO exhibited a good tendency for acetone oxidation in the presence of NH_3 and methanol gases [17]. The CuO nanoparticles supported on γ-Al_2O_3, pillared clay, and TiO_2 were used as catalysts for phenols oxidation in aqueous phases. The largest amount of produced CO_2 and the lowest amount of Cu leaching were in the presence of CuO/γ-Al_2O_3 nano-catalyst. It was also the most economically favorable catalyst [18].

In this research, a kinetics study of the acidic oxidation of acetone is carried out in the absence and presence of CuO nanoparticles supported on γ-Al_2O_3. The CuO amount varies by 0 (only γ-Al_2O_3), 2.5, 5, and 10% weights of the catalyst, and the kinetic parameters of the reaction are evaluated in their presence. The reaction rate laws are assumed as $Rate = k[A]^x$, and the data related to reactant concentrations versus time extracted and diagrams of $[A]^{-1}$, $[A]^{1-x}$, and $\ln[A]$ versus time are plotted so as to find a linear relationship. Afterward, the relationship between the rate constants and temperature is investigated through *Arrhenius* equation to find activation energies of the reactions.

2. Experimental

2.1. Materials

Sulfuric acid 98%, acetone, and potassium permanganate as reactants were purchased from Merck. $Cu(NO_3)_2.3H_2O$ was purchased from Sigma-Aldrich and used as a CuO precursor. Condea Vista Catalox γ-alumina with 212.4 $m^2.g^{-1}$ specific surface area and sodium oxide (Na_2O) $<$ 0.05 (ppm), Silica (SiO_2) $<$ 0.9 (ppm), Sulfate (SO_4) $<$ 1.5 (ppm) impurities was provided and treated. Deionized water was used as the water content of the reaction medium.

2.2. Methods

2.2.1. Catalyst preparation

Catalysts were prepared via the impregnation method. Firstly, gamma alumina was treated in a laboratory furnace at 400°C to burn and remove possible organic impurities. Suitable solutions of $Cu(NO_3)_2.3H_2O$ were prepared in deionized water. For the preparation of CuO/γ-Al_2O_3 with 2.5, 5, and 10% weights of CuO, the prepared solutions were added to γ-Al_2O_3 and heated for water evaporation and to make a sludge. The sludges were dried at 120°C for 2 h and, then, calcined at 400°C for 4 h for the CuO phase formation.

2.2.2. Catalyst characterization

After calcination, the catalysts were analyzed using ICP-OES, XRD, BET, and TEM to determine their characteristics. The CuO loading amounts on γ-Al_2O_3 were analyzed by Varian VISTA-MPX inductively coupled plasma-optical emission spectrometry (ICP-OES) instrument. The XRD patterns of catalysts were obtained with X'Pert Philips type: 3040/60 X-ray diffractometer with monochromatized Cu/Kα radiation. The surface area, pore volume, and average pore sizes of catalysts that are effective parameters in catalytic performance were measured by BELSORP-mini II, MicrotracBEL Company, Japan. For this purpose, samples were degassed at 200°C for 4 h under 50 mTorr vacuum, and the parameters were determined. Transmission electron microscopy, TEM, (Philips CM20, 100kV, equipped with a NARON energy dispersive spectrometer with germanium detector) was used to illustrate the presence of particles in the bulk of nano-porous support. Samples for TEM micrographs were treated by ultrasonic dispersion in ethanol. The suspensions were dropped onto a carbon-coated copper grid.

2.2.3. The experiment procedure

To determine the order of the reaction based on Relation (1) and Eq. (2), in the absence and presence of CuO/γ-Al_2O_3 catalysts, the concentration of one reactant was much less than that of others. The reaction was performed at 25°C and atmospheric pressure. Specified volumes of reaction mixture were sampled at specific time reactions, and the remaining potassium permanganate was detected by the UV-VIS spectrometer at a wavelength of 526 nm. Experiments done for calculating E_a were carried out by modifying the temperature and detecting the remaining potassium permanganate at different specific reaction times. To find a probable linear relationship between time and concentration, diagrams of $[A]^{-1}$, $[A]^{1-x}$, and $\ln[A]$ versus time are plotted.

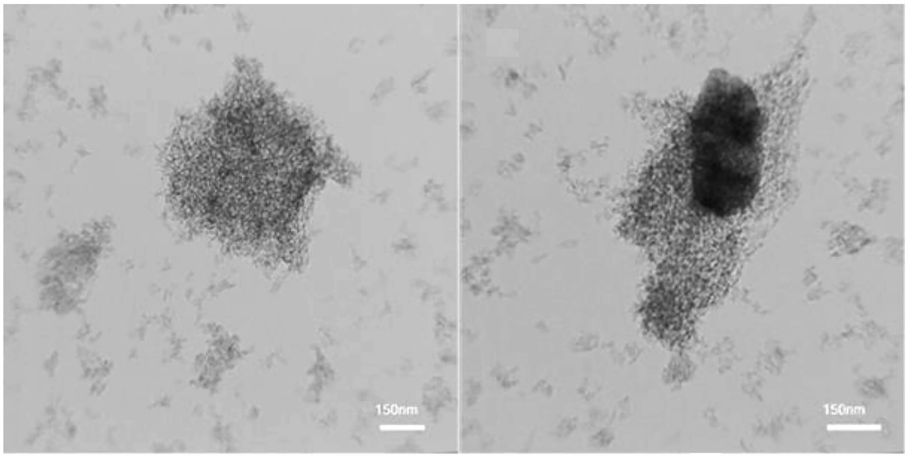

(a) (b)

Figure 1. TEM micrographs of (a) γ-Al_2O_3 and (b) CuO/γ-Al_2O_3 with 10 wt% of CuO as the best catalyst.

Table 1. The results of ICP-OES analysis of calcined catalysts.

Catalysts	Catalyst name	Expected values (wt%)	ICP-OES values (wt%)
γ-Al_2O_3	CuO-0	0	0
CuO/γ-Al_2O_3-2.5wt%	CuO-2.5	2.5	2.46
CuO/γ-Al_2O_3-5wt%	CuO-5	5	4.93
CuO/γ-Al_2O_3-10wt%	CuO-10	10	9.88

$$6KMnO_4 + 9H_2SO_4 + 5(CH_3)_2CO \rightarrow 3K_2SO_4 + 6MnSO_4 + 5CH_3COOH + 5HCOOH + 9H_2O, \quad (1)$$

$$\text{Rate} = k[KMnO_4]^n[H_2SO_4]^m[(CH_3)_2CO]^l [K_2SO_4]^k[MnSO_4]^x[CH_3CHOOH]^y[HCOOH]^z. \quad (2)$$

Activation energies of the reactions were calculated based on *Arrhenius* equation (Eq. (3)), which depicts the interdependence of temperature and rate constant. It has been empirically observed that if the temperature range is in a narrow range, the logarithm of the rate constant with changes in T^{-1} linearly changes and the line slope is negative. In this term, if the logarithm of the rate constant is equal to T^{-1}, then E_a has no dependence on T. The factor A is the number of collisions per unit time and volume unit, yet not for all collisions. The factor holds for those collisions that are in the right direction and have enough energy to reach the peak. If the constant of the reaction rate follows the *Arrhenius* equation, it can be calculated based on other parameters of *Arrhenius* equation by measuring the reaction rate constant at different temperatures.

$$\frac{d\ln k}{dT} = \frac{E_a}{RT^2}, k = Ae^{(-E_a/RT)}. \quad (3)$$

3. Results and discussion

3.1. Catalyst characterization

The ICP-OES was used to determine CuO amounts that were impregnated on γ-Al_2O_3. Results are reported in Table 1. As shown in the table, the values of impregnated metals are very close to the expected ones.

Figure 1 shows TEM micrographs of γ-Al_2O_3 (a) and CuO/γ-Al_2O_3 (b) with 10 wt% of CuO as a catalyst with the best performance. The figure clearly shows the nano-porous structure of γ-Al_2O_3 and approves the favorable incorporation of CuO particles with nano sizes and porous support.

The XRD patterns of γ-Al_2O_3 and CuO/γ-Al_2O_3 with different CuO amounts are shown in Figure 2. Peaks at $2\theta = 35.5$, 38.7, 49.1 and peaks at $2\theta = 37.4$, 45.9, 61.6, and 66.6 are related to CuO and γ-Al_2O_3, respectively.

The surface characterization results of all catalysts are reported in Table 2. Results of BET surface area (S_{BET}) showed that, in all cases, the addition of metal oxide to γ-Al_2O_3 reduced the S_{BET} of the catalysts. Pore volume and average pore diameter also decreased with the increasing CuO loading. Pore blockage by loaded CuO is responsible for this increase.

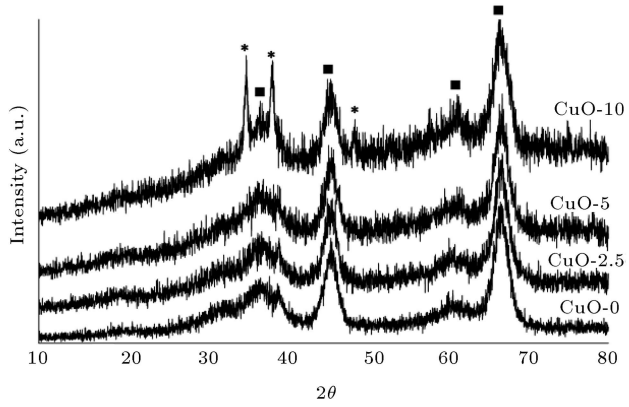

Figure 2. The XRD patterns of γ-Al_2O_3 and CuO/γ-Al_2O_3 with different CuO amounts: (■) γ-Al_2O_3 and (*) CuO.

Table 2. The textural properties of γ-Al_2O_3 and CuO/γ-Al_2O_3 with different CuO amounts.

Sample	S_{BET} ($m^2.g^{-1}$)	Pore volume ($ml.g^{-1}$)	Average pore diameter (A)
CuO-0	212.43	0.6653	145.06
CuO-2.5	197.07	0.6411	138.74
CuO-5	184.31	0.6192	133.92
CuO-10	173.14	0.5346	124.58

3.2. Order of the reaction for reactants and products

To find the order of the reaction for $KMnO_4$, a solution was prepared using acetone, $KMnO_4$ and H_2SO_4 with concentrations of 0.206, 0.00486, and 0.36 M, respectively. The $KMnO_4$ concentration was determined in time periods. Data were collected and diagrams were plotted. Results showed that there was a linear relationship between the reaction time and the logarithm of $KMnO_4$ concentration. Therefore, the obtained order of the reaction for potassium permanganate was one. For acetone, a solution was prepared using acetone, $KMnO_4$ and H_2SO_4 with concentrations of 0.0264, 0.0101, and 0.36 M, respectively. There was also a linear relationship between reaction time and the logarithm of acetone concentration. Therefore, the obtained order of the reaction for acetone was also one. Figure 3 shows the relationship between $KMnO_4$ and acetone concentrations over time.

For H_2SO_4, 10 solutions with H_2SO_4 concentrations of 0.36, 0.50, 1.00, 1.25, 1.50, 1.75, 2.00, 2.25, and 2.50 with the constant concentration of acetone and potassium permanganate were prepared. Results showed that there was a linear relationship between the concentration of H_2SO_4 and reaction rate. Therefore, the obtained order of reaction for H_2SO_4 was one. Figure 4 shows diagrams of the order of the reaction for H_2SO_4.

To determine the order of the reaction for products, solutions with constant concentrations of acetone (0.206 mole.L^{-1}), $KMnO_4$ (0.0035 mole.L^{-1}), and H_2SO_4 (1.00 mole.L^{-1}) and different $MnSO_4$ concentrations were prepared as the reaction medium. The remaining $KMnO_4$ was detected at the same reaction times and results are shown in Table 1. It was observed that there was no relationship between $MnSO_4$ concentration and reaction rate. To illustrate the dependence of the reaction rate on K_2SO_4, acetic acid, and formic acid concentrations, similar experiments were designed and, thus, similar results were obtained. Therefore, the reaction rate law becomes as follows:

$$Rate = k[KMnO_4]^1[H_2SO_4]^1[(CH_3)_2CO]^1.$$

3.3. Activation energy of the non-catalytic reaction

Ten same solutions as reaction media were prepared with acetone and $KMnO_4$ and H_2SO_4 concentrations of 0.206, 0.005, and 1.00 mole.L^{-1}, respectively. Reaction was carried out at ten different temperatures, and the remaining $KMnO_4$ was detected at different time reactions. The initial rate and rate constant were calculated according to the initial concentrations and reaction rate law in the time range at different temperatures. Diagram of ln k versus inverse temperature was plotted (Figure 5), and $-Ea.R^{-1}$ and -ln A were evaluated according to the line equation, as shown in Table 3.

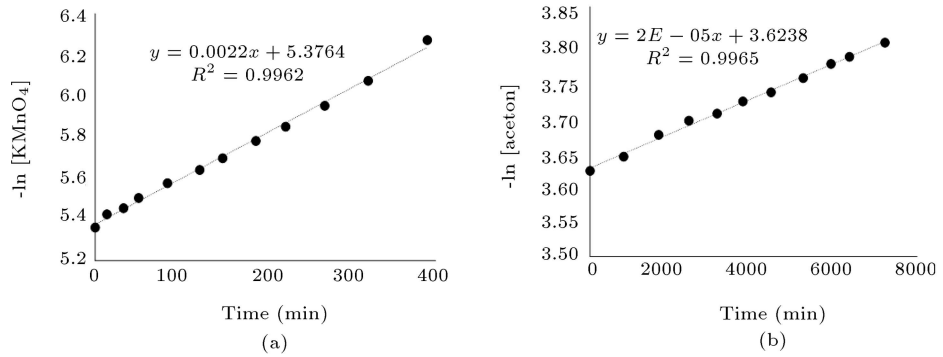

Figure 3. Linear relationship between (a) –ln [$KMnO_4$] and (b) –ln [acetone] and time.

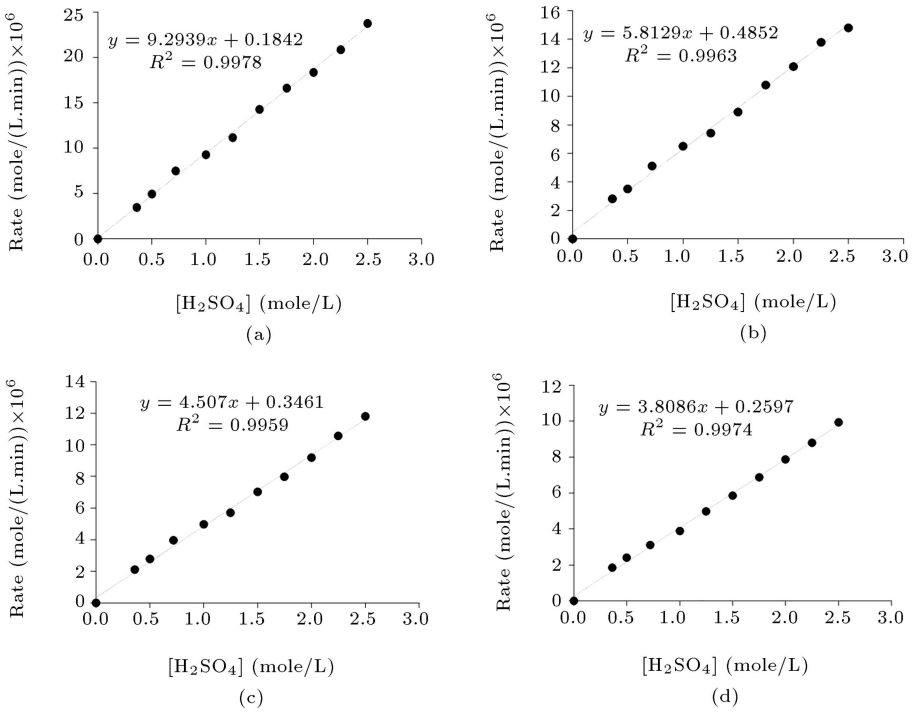

Figure 4. The rate of reaction versus initial H_2SO_4 concentration for the first (a) 25, (b) 50, (c) 75, and (d) 100 minutes.

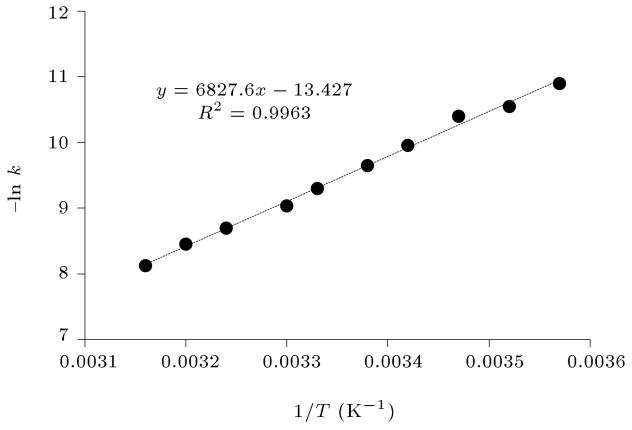

Figure 5. Linear function of –ln k vs T^{-1} confirms that the constant of the reaction rate in the absence of heterogeneous catalysts follows the *Arrhenius* equation.

Table 3. *Arrhenius* equation parameters extracted from –ln k vs T^{-1} diagram for reaction in the absence of heterogeneous catalysts.

E_a/R	E_a (kJ)	ln A	$A\left(\frac{L^2}{mol^2.s}\right)$
6827.6	56.767	13.427	678017

3.4. Effect of CuO/γ-Al_2O_3 on Arrhenius parameters

To determine the effect of prepared catalysts on *Arrhenius* parameters, the same experiments shown in Section 3.3 were designed and performed in the presence of CuO-0, CuO-2.5, CuO-5, and CuO-10. Table 4 shows the *Arrhenius* parameters of the reaction in the presence of catalysts. Figure 6 also shows the linear relationship between -ln k and inverse temperature for all catalysts. Figure 7 compares the activation energies for reaction in the absence and presence of CuO/γ-Al_2O_3.

Table 4. *Arrhenius* equation parameters extracted from –ln k vs $1.T^{-1}$ diagram.

Catalyst	E_a/R	E_a (kJ)	ln A	$A\left(\frac{L^2}{mol^2.s}\right)$
CuO-0	6832.7	56.807	13.458	699415
CuO-2.5	6492.5	53.978	12.492	266199
CuO-5	6023	50.075	11.414	90581
CuO-10	5626.7	46.777	10.620	40945

According to the results, reaction in the presence of γ-Al_2O_3 (CuO-0) had slightly higher activation energy than non-catalytic one. It can be related to the fact that γ-Al_2O_3 has no notable catalytic effect on the reaction of acetone acidic oxidation with $KMnO_4$, like many other reactions. Actually, γ-Al_2O_3 is used as catalyst support because of amphoteric and inert behavior in the reaction medium and the high surface area for metal or metal oxide distribution [19]. However, the reaction had slightly greater activation energy in the presence of γ-Al_2O_3 than non-catalytic reaction, which can be attributed to the homogeneity of the reaction medium in the non-catalytic one. The γ-Al_2O_3 creates a heterogeneous medium for reaction and can limit the mass transfer of reactants during the reaction. Therefore, higher activation energy is

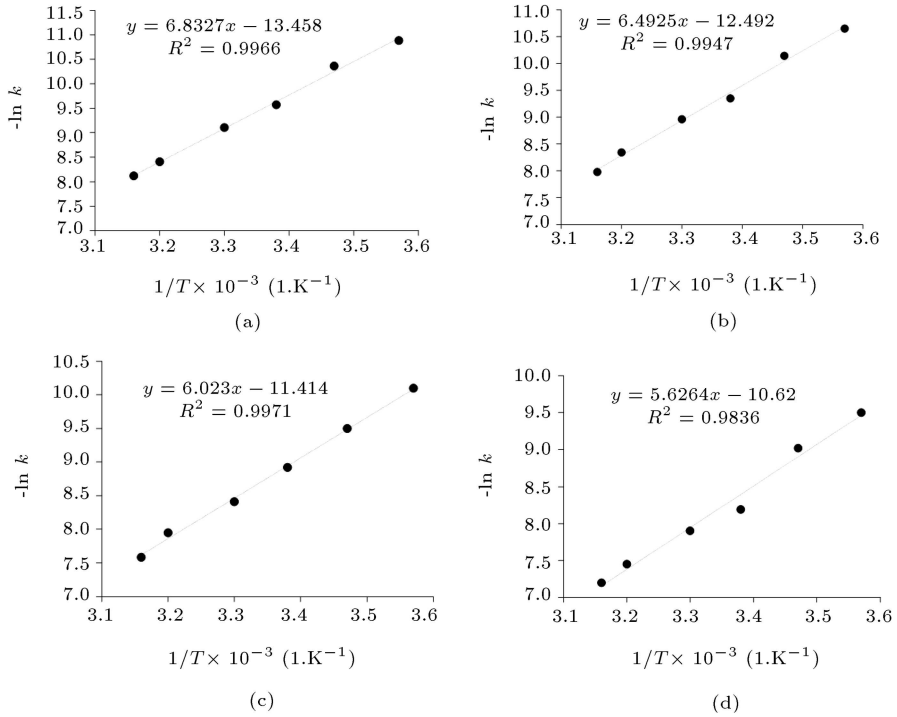

Figure 6. The linear relationship between –ln k and inverse temperature for (a) CuO-0, (b) CuO-2.5, (c) CuO-5, and (d) CuO-10.

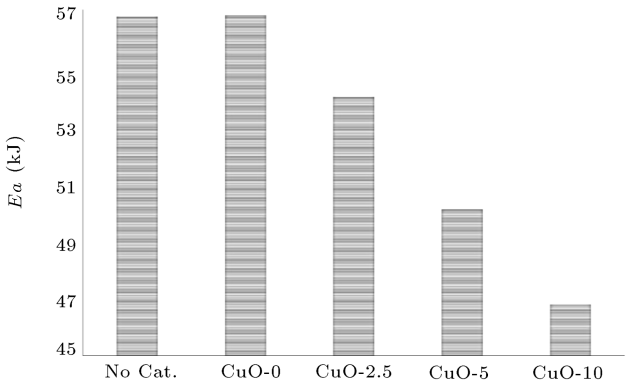

Figure 7. The activation energies for reaction in the absence and presence of different concentrations CuO on the catalyst.

required for the reaction progress. With the addition of CuO concentration to γ-Al_2O_3, the activation energy started to decrease. It is related to the catalytic effect of CuO on acidic oxidation of acetone in the presence of $KMnO_4$. Figure 8 shows the suggested mechanisms for acidic acetone oxidation with $KMnO_4$ on CuO nano-catalyst. According to similar studies, two mechanisms can be suggested. Since the reaction mechanism of ketones oxidation contains enol creation as intermediates, the intermediate is 2-hydroxypropene in case of acetone oxidation, and it appears that CuO facilitates the C=C bond adsorption on the catalyst surface and makes enols more stable (Figure 8(a)). Therefore, the formation of the activated complex requires less energy than that in the non-catalytic process. On the other hand, it has been reported that CuO has catalytic effect on oxygenates (alcohols and ethers) production from syngas or sugar precursors [20]. The effect is associated with the tendency of CuO to C-O group adsorption. Therefore, C-O group of enols also can be adsorbed on CuO surface, which can be another reason for enol stability in the presence of this catalyst. More stable intermediate needs less activation energy. The description of another mechanism is based on $MnO4^-$ adsorption on CuO surface. Since MnO_4^- has negative charge, it can interact with half-filled orbital of CuO. More CuO sites on the catalyst surface cause more interactions with MnO_4^- and, subsequently, more enol oxidation (Figure 8(b)). Therefore, the tendency of MnO_4^- to be adsorbed on CuO surface deceases the activation energy.

4. Conclusion

A kinetic study of acidic oxidation of acetone with $KMnO_4$ in the absence and presence of CuO supported on a nano-porous structure of γ-Al_2O_3 was carried out. There were linear relationships between the reaction time and the logarithms of acetone and $KMnO_4$ concentrations and, also, between the concentration of H_2SO_4 and the reaction rate. Therefore, the reaction order for all of them was measured to be one. There was no relationship between the product concentrations and the rate of the reaction. Results showed a

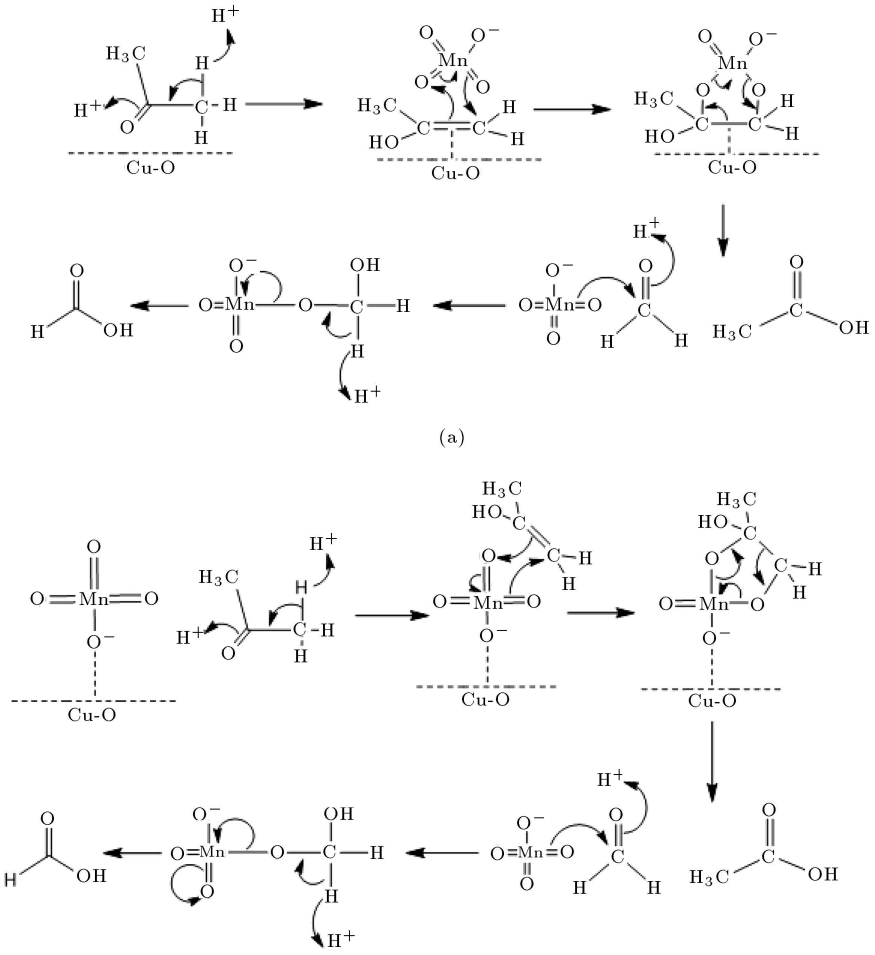

Figure 8. The suggested mechanisms for acidic acetone oxidation with potassium permanganate in the presence of CuO.

significant catalytic effect of CuO in this reaction. It was demonstrated that the 10 wt% increase of CuO in catalyst formula decreased 17.5% of activation energy of the reaction, which corresponded to the tendency of CuO to the adsorption of species with C=C and C-O functional groups. As the enols are intermediates in the ketone oxidation mechanism, these adsorptions make 2-hydroxypropene more stable on the catalyst surface. The stability of intermediates causes lower activation energy requirement. The adsorption of MnO_4^- on CuO surface because of the interaction between the negative charge and half-filled orbital of CuO and, subsequently, the oxidation of enols can be another way for acetone oxidation. Therefore, the CuO/γ-Al_2O_3 nano-catalyst, which is an inexpensive material, can be good candidate for a heterogeneous catalyst for the acidic oxidation of acetone with $KMnO_4$.

References

1. Dilsha, K. and Kothari, S. "Kinetics and mechanism of the oxidation of some thioacids by butyltriphenylphosphonium dichromate", *Progress in Reaction Kinetics and Mechanism*, **32**, pp. 119–129 (2007).

2. Goyal, A., Kothari, S., and Banerji, K.K. "Kinetics and mechanism of the oxidation of substituted benzyl alcohols by butyltriphenylphosphonium dichromate", *Journal of Chemical Research*, **2002**, pp. 363–365 (2002).

3. Pandey, D. and Kothari, S. "Kinetics and correlation analysis of reactivity in the oxidation of aromatic aldehydes by butyltriphenylphosphonium dichromate", *Progress in Reaction Kinetics and Mechanism*, **33**, pp. 293–311 (2008).

4. Likhodii, S.S., Serbanescu, I., Cortez, M.A., et al. "Anticonvulsant properties of acetone, a brain ketone elevated by the ketogenic diet", *Annals of Neurology*, **54**, pp. 219–226 (2003).

5. Zhao, Q., Ge, Y., Fu, K., et al. "Oxidation of acetone over Co-based catalysts derived from hierarchical layer hydrotalcite: Influence of Co/Al molar ratios and calcination temperatures", *Chemosphere*, **204**, pp. 257–266 (2018).

6. Zhang, C., Wang, J., Yang, S., et al. "Boosting total oxidation of acetone over spinel MCo_2O_4 (M= Co, Ni, Cu) hollow mesoporous spheres by cation-substituting effect", *Journal of Colloid and Interface Science*, **539**, pp. 65–75 (2019).

7. Yuan, Z.T.C.M.G. and Xiao-Ming, Y.Z. "0.1% Pt-0.02% Pd/Stainless steel monolith catalyst: catalytic oxidation of acetone and thermal stability", *Chinese Journal of Inorganic Chemistry*, **8**, p. 009 (2010).

8. Zarczynski, A., Gorzka, Z., Zaborowski, M., et al. "Oxidation of the mixture acetone-water (1: 5) containing of 2, 4-dichlorophenoxyacetic acid with application of monolithic platinum-rhodium catalyst", Ecological Chemistry and Engineering S-chemia I Inzynieria Ekologiczna S, **16**, pp. 107–113 (2009).

9. Gandıa, L., Vicente, M., and Gil, A. "Complete oxidation of acetone over manganese oxide catalysts supported on alumina-and zirconia-pillared clays", *Applied Catalysis B: Environmental*, **38**, pp. 295–307 (2002).

10. Samad, S., Loh, K.S., Wong, W.Y., et al. "Carbon and non-carbon support materials for platinum-based catalysts in fuel cells", *International Journal of Hydrogen Energy*, **43**, pp. 7823–7854 (2018).

11. Barati, M. and Kahid Baseri, G. "Hydrogen, alcohols, and ethers production from biomass in supercritical methanol-subcritical water medium with Cu-K nanocatalysts", *Environmental Progress & Sustainable Energy*, **37**, pp. 861–869 (2018).

12. Parmeggiani, C., Matassini, C., and Cardona, F. "A step forward towards sustainable aerobic alcohol oxidation: new and revised catalysts based on transition metals on solid supports", *Green Chemistry*, **19**, pp. 2030–2050 (2017).

13. Iwamoto, H., Kameoka, S., Xu, Y., et al. "Effects of Cu oxidation states on the catalysis of NO+ CO and N2O+ CO reactions", *Journal of Physics and Chemistry of Solids*, **125**, pp. 64–73 (2019).

14. Wu, K., Fu, X.-P., Yu, W.-Z., et al. "Pt-Embedded CuO x-CeO_2 multicore-shell composites: interfacial redox reaction-directed synthesis and composition-dependent performance for CO oxidation", *ACS Applied Materials & Interfaces*, **10**, pp. 34172–34183 (2018).

15. Momeni, S. and Sedaghati, F. "CuO/Cu_2O nanoparticles: A simple and green synthesis, characterization and their electrocatalytic performance toward formaldehyde oxidation", *Microchemical Journal*, **143**, pp. 64–71 (2018).

16. Subramanian, E. and Subbulekshmi, N. "Enhanced heterogeneous wet hydrogen peroxide catalytic oxidation performance of fly ash-derived zeolite by CuO incorporation", *Scientia Iranica, Transaction C, Chemistry, Chemical Engineering*, **24**, p. 1189 (2017).

17. Hien, V.X., Minh, N.H., Son, D.T., et al. "Acetone sensing properties of CuO nanowalls synthesized via oxidation of Cu foil in aqueous NH_4OH", *Vacuum*, **150**, pp. 129–135 (2018).

18. Pires, C.D., Dos Santos, A., and Jordão, E. "Oxidation of phenol in aqueous solution with copper oxide catalysts supported on γ-Al_2O_3, pillared clay and TiO_2: comparison of the performance and costs associated with each catalyst", *Brazilian Journal of Chemical Engineering*, **32**, pp. 837–848 (2015).

19. Cordi, E.M. and Falconer, J.L. "Oxidation of volatile organic compounds on Al_2O_3, Pd/Al_2O_3, and PdO/Al_2O_3Catalysts", *Journal of Catalysis*, **162**, pp. 104–117 (1996).

20. Matson, T.D., Barta, K., Iretskii, A.V., et al. "One-pot catalytic conversion of cellulose and of woody biomass solids to liquid fuels", *Journal of the American Chemical Society*, **133**, pp. 14090–14097 (2011).

Biographies

Mohammad Taha Badri received a BSc degree from Shahid Rajaee University and a MS degree in Physical Chemistry from Kharazmi University in Tehran. He is a PhD student at Kashan University. His research field is about statistical mechanics and the study of thermodynamic quantities. The calculation of internal energy is based on the Ising model on a two-layer square lattice as a sample of his research work. Currently, his subject matters of interest cover the chemical kinetics and obtaining kinetic parameters and determining the mechanism.

Mohammad Barati is a faculty member of Kashan University who works in the field of Applied Chemistry. Most of His research topics cover the field of gaseous, liquid, and solid fuels produced from bioresources. Biodiesel production from algae and other oily biomasses in supercritical conditions is also included. Water, methanol, hexane, and acetone in supercritical conditions are used for biomass conversion to biofuels in the Lab. Nanocomposites for bio applications are his other field of research. Chemicals from medicinal herbs are considered for applying to the controlled drug delivery systems, especially polymer nanocomposites. Recent studies have also researched the production of biodiesel from algae and other oily biomasses under supercritical conditions. His PhD thesis is focused on the production of hydrogen gas from biomass feedstock using catalytic sub and supercritical water gasification. Ni, Ru, Cu, and K are the metals he is working on. His MSc thesis is focused on inhibiting the steel electrochemical corrosion with polymer nanocomposite

coatings. The polymer matrix contains polyaniline as an electroactive polymer and Zn metal nanoparticles applied as an additive.

Sayyed Hossein Rasa is a faculty member of Kashan University who works in the field of Physical Chemistry. Most of His research topics cover the field of thermodynamics and kinetics. A study of two-phase systems, theoretical and empirical analysis of liquid-liquid systems of liquid systems, kinetic studies, and the provision of a mechanism such as the kinetic study of sulfite ion oxidation, enzymatic reactions, hydroquinone oxidation and reactive oxygen species in several systems using simulation are a few examples of his research work. Recent studies have also researched the synthesis and properties of nanostructures.